

M. CIEŚLA*[#], G. JUNAK*, J. TOMCZAK**[#], R. FINDZIŃSKI*, T. KAWAŁA***

DURABILITY OF X10CrMoVNb9-1 STEEL TUBES UNDER LOW-CYCLE FATIGUE AND CREEP CONDITIONS AFTER BENDING WITH LOCAL INDUCTION HEATING

TRWAŁOŚĆ W WARUNKACH ZMĘCZENIA NISKOCYKLOWEGO I PEŁZANIA MATERIAŁU RURY ZE STALI X10CrMoVNb9-1 PO PROCESIE GIĘCIA Z LOKALNYM NAGRZEWEM INDUKCYJNYM

The paper contains the results of theoretical and experimental research on the tube bending process used in the manufacturing of X10CrMoVNb9-1 steel tubes with dimensions 530 x 90 mm. An innovative technology in which the tube bending is coupled with local induction heating and the results of finite-element numerical modelling of tube bending using Simufact Forming 11.0 software are presented. A change of the geometry in the cross-section of the bend area was subjected to analysis, including the ovalization of the cross-section and the wall thickness in the regions subject to tension and compression. The geometrical features of the bend determined on the basis of numerical calculations were compared with the measurement results obtained in industrial conditions. Basic mechanical properties of the tube in the as-delivered condition and of the fabricated tube bend were determined using tensile, hardness, impact, low-cycle fatigue and creep tests. It was proved that the tube bend made of the X10CrMoVNb9-1 steel, obtained by the proposed technology, meets the requirements of the applicable standards.

Keywords: tube bending, numerical modelling, mechanical properties, creep, low-cycle fatigue

W artykule zawarto wyniki analizy teoretycznej i doświadczalnej procesu gięcia rur ze stali X10CrMoVNb9-1 o wymiarach 530 x 90 mm. Przedstawiono innowacyjną technologię procesu gięcia rur z lokalnym nagrzewaniem indukcyjnym oraz wyniki modelowania numerycznego kształtowania łuku rurowego metodą elementów skończonych z użyciem programu Symufact Forming 11.0. Analizowano zmianę geometrii na przekroju poprzecznym łuku w tym; owalizację przekroju, grubość ścianek w strefie rozciąganej i ściskanej. Cechy geometryczne łuku określone na podstawie obliczeń numerycznych porównano z wynikami pomiarów w warunkach przemysłowych. Określono podstawowe właściwości mechaniczne rury w stanie dostawy i wykonanego łuku na podstawie przeprowadzonych prób; rozciągania, twardości, uderności, zmęczenia niskocyklowego i pełzania. Wykazano, że wykonany łuk rurowy ze stali X10CrMoVNb9-1 gięty zaproponowaną technologią spełnia wymagania odpowiednich norm.

1. Introduction

The construction of modern 1000MW supercritical coal-fired boilers is the main direction for power industry development in the current decade. The most modern materials, such as X10CrMoVNb9-1 or X10CrWMoVNb9-2 steels, must be taken into consideration in the design process for this kind of devices. These materials must be able to meet very high requirements in terms of the efficiency and availability expected by the user [1-5]. This applies especially to steam pipelines, which operate at a temperature equal or higher than 600°C and under pressure exceeding

28MPa. These objects are exposed mainly to the harmful effects of progressive changes in the material caused by, among others, creep processes and, in many cases, processes of thermo-mechanical fatigue of a low-cycle nature [2, 4, 6, 7, 8].

Tube bends [9-11] are used in practically all power pipelines. Therefore, unconventional bending methods, including those using local heating of tubes during forming [12], are finding application in their production technology more and more often. A diagram of the tube bending with a local induction heating is shown in Fig. 1.

* SILESIA UNIVERSITY OF TECHNOLOGY, FACULTY OF MATERIALS ENGINEERING AND METALLURGY, DEPARTMENT OF METALS TECHNOLOGY, 8 KRASIŃSKIEGO STR., 40-019 KATOWICE, POLAND

** LUBLIN UNIVERSITY OF TECHNOLOGY, FACULTY OF MECHANICAL ENGINEERING, DEPARTMENT OF COMPUTER MODELLING AND METAL FORMING TECHNOLOGIES, 36 NADBYSZYCKA STR., 20-128 LUBLIN, POLAND

*** ZRE KATOWICE S.A. PRODUCTION CENTRE, 2 MARTYNIAKÓW STR., 43-603 JAWORZNO, POLAND

[#] Corresponding author: marek.ciesla@polsl.pl

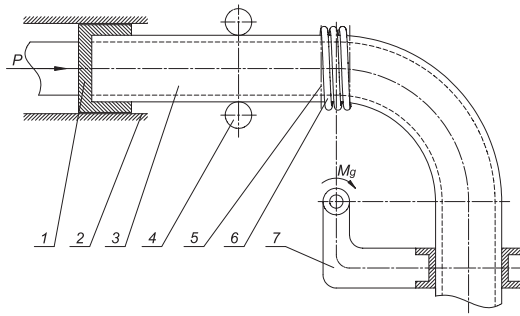


Fig. 1. Diagram of a device for tube bending with local induction heating: 1 – fixing element, 2 – feed mechanism guides, 3 – tube subject to bending, 4 – guiding rollers, 5 – heating and forming zone, 6 – coil, 7 – forming arm, P – pushing force, Mg – bending moment

The authors find it appropriate to undertake research oriented towards the determination of relations between the technological parameters of the tube bending process and the mechanical properties of the tube bend material, which should not diverge from the properties of the tube in its initial state (as delivered). Examination of the basic mechanical properties, as well as low-cycle fatigue and creep tests at a temperature of 600°C have been carried out.

The test material consisted of a high-temperature creep resisting steel X10CrMoVNb9-1 tube with dimensions 530x90 mm, which was thermally treated through normalization and tempering (heat treatment of NT type) and a tube bend made of this steel, formed at 950°C, with bending radius 1325 mm, which was thermally treated through toughening (heat treatment of QT type). Industrial trials of forming tube bends were performed at Zakłady Remontowe Energetyki Katowice S.A.

2. Numerical modelling of the tube bending process

Forming of a tube bend made of the X10CrMoVNb9-1 steel, with the dimensions 530x90 mm and bending radius 1325 mm, was modelled. Calculations by means of the finite-element method (FEM) were conducted using the Simufact Forming software, version 11.0. This software was repeatedly used for numerical modelling of complex metal forming processes and the obtained results were successfully verified experimentally [13–16].

Numerical simulations of the tube bending process were carried out in the range of heating temperature of 900 - 1050°C at a feed rate of the pusher: 2.5 – 5.0 mm/min. The model of the material was developed based on plastometric compression tests and the examples of the flow curves are shown in Fig. 2. It was assumed in the numerical simulation that a semi-finished product was heated right through along a 60 mm long segment, up to the forming temperature. The assumed initial temperature of the semi-finished product, the environment and tools, was 20°C. The other parameters adopted for the calculations were as follows: the factor of friction between the semi-finished product and tools $m = 0.3$ (constant friction model), material/tool heat exchange coefficient – 10 kW/m²K, heating ring/semi-finished product heat exchange coefficient – 100 kW/m²K, material/environment heat exchange coefficient – 0.35 kW/m²K for cooling in standing air.

The optimal geometry of the bend in its cross- and longitudinal section, determined using FEM, is shown in Fig. 3. Measurements of geometrical parameters were taken in five cross-section (marked in Fig. 3), perpendicular to the bend's axis. The shape of the tube bend is characterised by slight ovalization of the section (ca. 0.8%, Table 1). An increase in the wall thickness was observed within the internal area of the bend, where compressive stresses predominate, and thinning of the walls within the external area, where tensile stresses prevail. When analysing the strain distribution, it is visible that the strain is not homogeneous. The highest plastic strain is present within the internal radius zone (circa 0.3), while the area of occurrence of similar strain values within the external radius zone is much smaller.

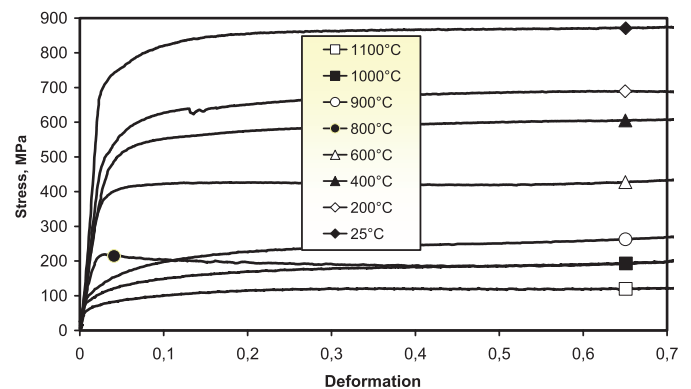


Fig. 2. Flow curves determined for the X10CrMoVNb9-1 steel in plastometric compression tests

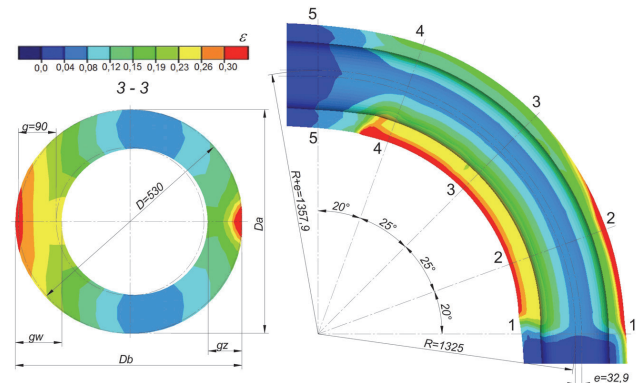


Fig. 3. Change in the tube bend's section geometry determined using FEM (heating temperature: 950°C)

The factor that initiates forming in induction bending processes is the temperature, which decreases the plastic flow resistance in the bending zone, owing to which the material is deformed over a relatively short segment. Therefore, during the FEM analysis the temperature distribution was also taken into account. The temperature distributions determined by FEM and the Cockcroft-Latham fracture criterion are presented in Fig. 4. The temperature distribution within the forming area is not of a homogenous nature. Directly in the heating ring area, the temperature reaches the assumed values (ca. 950°C). Farther on from the heating zone, the temperature drops quickly until reaching the ambient temperature.

TABLE 1

Geometrical parameters of the tubes subject to bending, obtained in FEM simulation (temperature 950°C)

Geometrical features of the tube						
tube diameter $D = 530$ mm, wall thickness of the tube $g = 90$ mm,						
Geometrical features of the bend						
bending radius $R = 1325$ mm, shift of the neutral axis $e = 32.9$ mm						
Bend section no.	1-1	2-2	3-3	4-4	5-5	Mean value
Wall thickness in the tensioned zone of the bend g_t [mm]	81.9	81.3	80.9	82.1	86.0	82.4
Wall thickness in the compressed zone of the bend g_w [mm]	107.7	108.6	108.9	108.8	107.5	108.3
Large axis of the ellipsis D_b [mm]	536.1	528.3	529.8	531.2	532.4	531.6
Small axis of the ellipsis D_a [mm]	531.5	532.2	532.9	533.2	533.6	532.7
Section ovalization e , %						
$e = \frac{D_a - D_b}{D} \cdot 100\%$	0.8	0.7	0.6	0.4	0.2	0.54

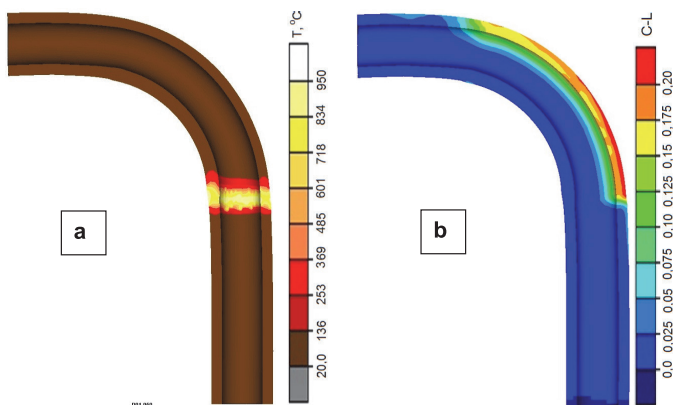


Fig. 4. FEM-determined distributions of: (a) – the temperature at the final stage of induction tube bending, (b) - Cockcroft-Latham failure criterion at the final stage of induction tube bending (optimal bending parameters)

The analysis of the Cockcroft-Latham failure criterion (Fig. 4b) shows that its highest values occur in the external radius zone of the tube bend. This is the area with the highest tensile stress which may lead to material cracking. The obtained Cockcroft-Latham integral values are relatively low (ca. 0.2). For typical constructional steels, threshold of the Cockcroft-Latham criterion adopts values within the range $0.7 \div 1$. The obtained results of numerical simulation of bending tubes made of X10CrMoVNb9-1 steel show that the resultant deformation (cross-section ovalization) is much lower than the admissible values. An increase of the heating temperature (within the range of $900^\circ - 1050^\circ$) affects the geometry of the formed bends to a small degree. The significant inhomogeneity of the obtained stress and strain distributions in the area of the bend formed affects the strength parameters of the tubes subject to bending. Therefore, the so-formed semi-finished products are subjected to heat treatment, the main purpose of which is to homogenize the mechanical properties within the

bending zone and in the non-deformed segments of the tube.

Optimal tube bending parameters, in terms of the geometrical features of the bend and force parameters of the bending process, as well as economic indicators, were defined, based on numerical simulations. The defined optimal tube bending parameters were applied in the process carried out in industrial conditions.

3. Industrial trial of induction tube bending

Forming of tube bends for power engineering applications was performed at Zakłady Remontowe Energetyki Katowice S.A. The parameters of bending and QT treatment (toughening) were selected based on numerical calculations, ZRE Katowice's own experiments and the PN-EN10216-2 standard. An induction bending machine was used, which enables tube bending in the range of diameters $D = 168.3 \div 1220$ mm with wall thickness of $g = 5 \div 100$ mm in the area of bending angles $\alpha = 0 \div 180^\circ$. A characteristic feature of the bend formed was a great compliance of its geometry with the outline determined in FEM numerical analysis. When analysing the geometry of the formed bend, a considerable change in the wall thickness can be observed (similar to that determined numerically), while the change in the wall thickness of the formed bend falls within the range acceptable by appropriate standards.

The minimum wall thickness in the tensioned zone amounted to $g = 80.9$ mm and was greater than the minimum thickness defined by the standard ($g = 60$ mm). At the same time, the measured minimum wall thickness of the bend in the compressed zone amounted to $g = 107.5$ mm and was greater than the minimum defined by the standard ($g = 72$ mm). Also, a slight deformation (ovalization) of the formed bend's cross-section occurred, whose maximum measured value was $e = 0.8\%$, which was much lower than the admissible $e = 8\%$.

4. Test results and their analysis

Evaluation of principal mechanical properties of a 530 x 90 mm tube in its as-delivered condition after heat treatment of NT type (normalizing and tempering) and of the bend formed from this tube after heat treatment of QT type (quenching and tempering), was performed based on the results of a tension, hardness and impact tests. Testing material was sampled from 3 zones of the tube bend and from tube.

The test results concerning the principal mechanical properties of the investigated materials are collated in Table 2. On the basis of their analysis it can be ascertained that the material of the bend formed from the X10CrMoVNb9-1 steel meets the requirements set forth in the PN-EN 10216-2 standard.

For selected zones of the bends and the as-delivered tube material, low-cycle fatigue tests were carried out. The tests simulated plastic deformation in the unsteady operation conditions of a power unit that is possible to occur in pipelines subject to the highest effort. The fatigue tests were conducted using a servo-hydraulic strength testing machine MTS on cylindrical specimens with a diameter of 12mm. The tests were conducted at an elevated temperature of 600°C with the machine being controlled by deformation at a constant frequency of the strain change of 0.1Hz. The tests were performed for the total strain range of $\Delta\epsilon_t = 0.6\%$ and 1.0%. Based on the results, the number of cycles until specimen's fracture (N_f) was determined. The developed characteristics of cyclic deformation and fatigue durability are shown in Fig. 5÷8. The recorded fatigue durability values, N_f , for the tube bend material were higher than for the tube material in the as-delivered condition, which indicates greater ability of the bend to transfer loads of a low-cycle nature. At the same time, amplitudal saturation stress σ_{an} of the bend material was lower (Fig. 5, 7). This testifies to the decrease of strength properties of the material in the conditions of cyclic loadings of an elastic-plastic nature.

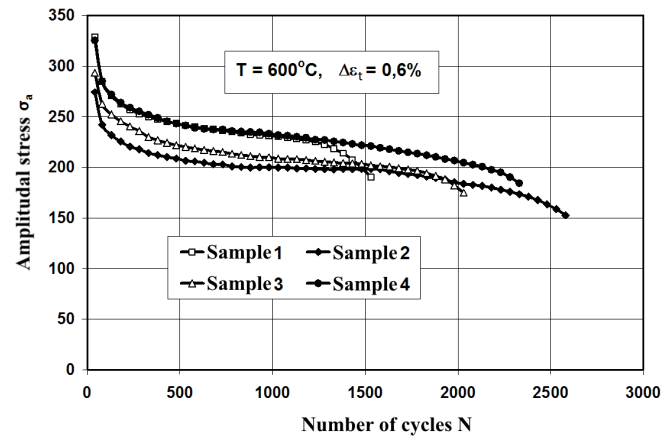


Fig. 5. Diagrams of cyclic deformation of the X10CrMoVNb9-1 steel tube material and of the tube bend

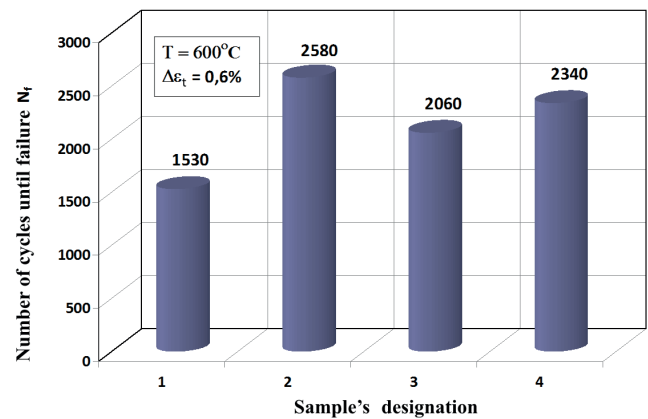


Fig. 6. Diagrams of low-cycle durability (N_f) of the X10CrMoVNb9-1 steel tube material and of the tube bend at a temperature of 600°C for the total strain range $\Delta\epsilon_t=0.6\%$

TABLE 2

Mechanical properties of the X10CrMoVNb9-1 steel tube and of the bend at room temperature

Sampling place	Sample design.	R_m MPa	$R_{p0.2}$ MPa	A5 %	Z %	KV J	HV10 kG/mm ²
tube: as-delivered	1	682.04	546.33	22.68	72.3	209	218.5
bend: straight segment behind the bend	2	638.43	492.95	25.38	73.85	194.3	214.3
bend: tensioned zone	3	649.83	500.6	24.97	75.03	192.2	209
bend: compressed zone	4	711.15	603.25	20.47	74.46	222.4	201.2
Properties in accordance with <i>PN-EN 10216-2</i>		630÷830	min 450	min. 19	-	min. 27	200÷260

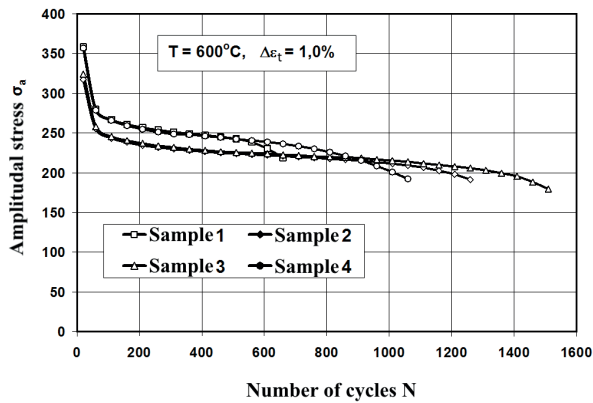


Fig. 7. Diagrams of cyclic deformation of the X10CrMoVNb9-1 steel tube material and of the tube bend

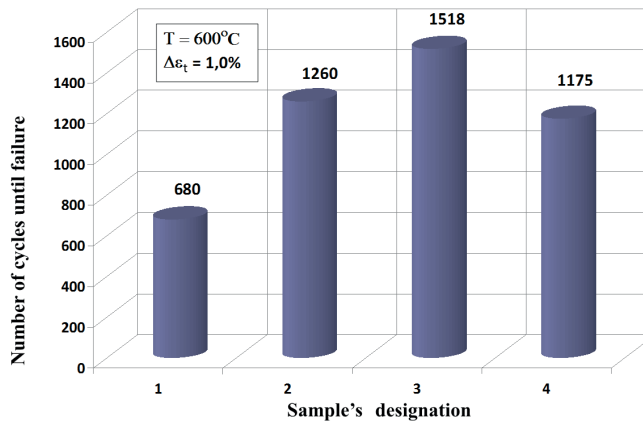


Fig. 8. Diagrams of low-cycle durability (N_f) of the X10CrMoVNb9-1 steel tube material and of the tube bend at a temperature of 600°C for the complete deformation range $\Delta\epsilon_t=1.0\%$

Creep tests were conducted to characterize the behaviour of the tube material in the steady operating conditions of a power installation. Creep tests of the materials presented in Table 2 were performed on an ATS-2330 machine in the Institute of Aviation, Warsaw. The tests were carried out at a temperature of 600°C under stress of 140 MPa. The developed characteristics of creep are shown in Fig. 9. The characteristics show considerably lower steady creep rates V_u

for the bend material compared to the tube material in its as-delivered condition. The effect thereof is higher creep durability (time until failure) of the bend material compared to the tube material in its as-delivered condition.

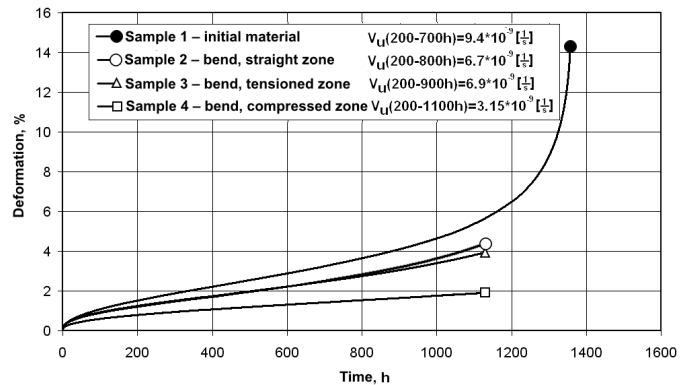
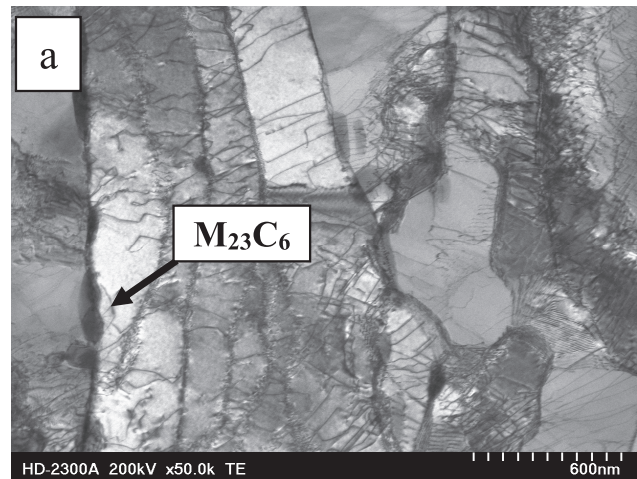
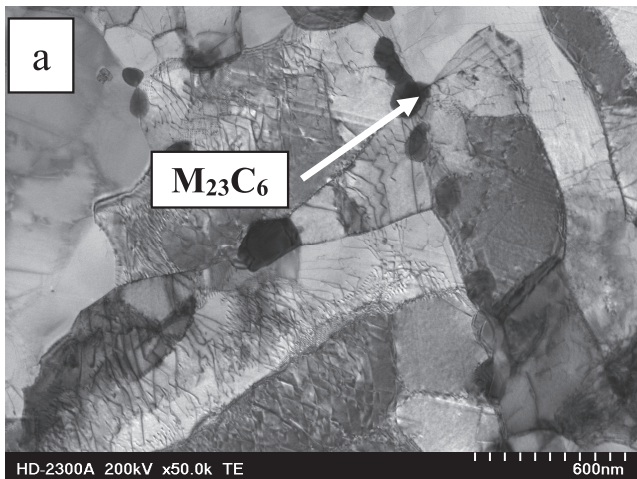


Fig. 9. Creep diagrams for the X10CrMoVNb9-1 steel tube material and bend at a temperature of 600°C and stress 140 MPa

To identify the potential cause of increase of the bend material durability compared to the tube as-delivered, examination of the materials' substructure was carried out using the thin-film technique. Observation of the substructure was performed on a transmission electron microscope. Observation of the tube material in the as-delivered condition and of the tube bend revealed dislocation structures and presence of carbides (mainly $M_{23}C_6$), as well as MX dispersion precipitates at grain boundaries and dislocations (Fig. 10 and 11). The tube material in its initial condition (Fig. 10) was characterized by a lower dislocation density and a higher ferrite subgrain size compared to the tube bend material after QT heat treatment (Fig. 11). It can be assumed that the observed differences in the microstructure of the tube in its initial condition (after type NT heat treatment) and of the bend (after QT heat treatment) resulted in the diversification of steady creep rates for the tested materials (Fig. 9). Both higher dislocation density and numerous subgrain boundaries contributed to strain consolidation of the bend material as a result of blocking of easy slip systems. [6] In consequence, the steady creep rate V_u of the bend has decreased (Fig. 9), which will result in its increased durability.



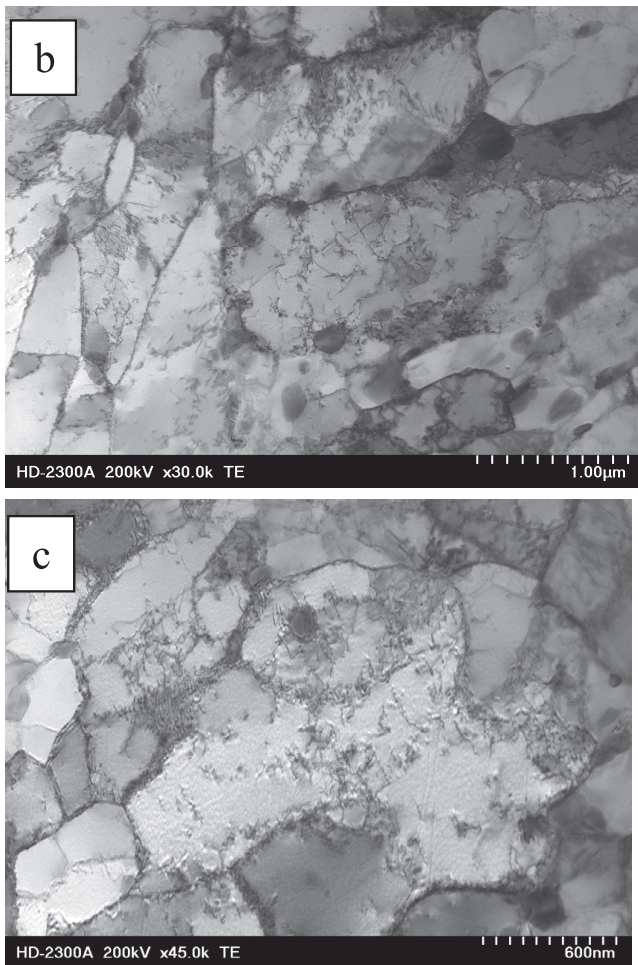


Fig. 10. Tempered martensite substructure of the tube material in its initial condition after NT heat treatment. Dispersion precipitates of M23C6 carbides are visible. Dislocation density is relatively lower in the subgrains, while the subgrain size is relatively larger compared to the bend material after QT heat treatment shown in Fig. 11

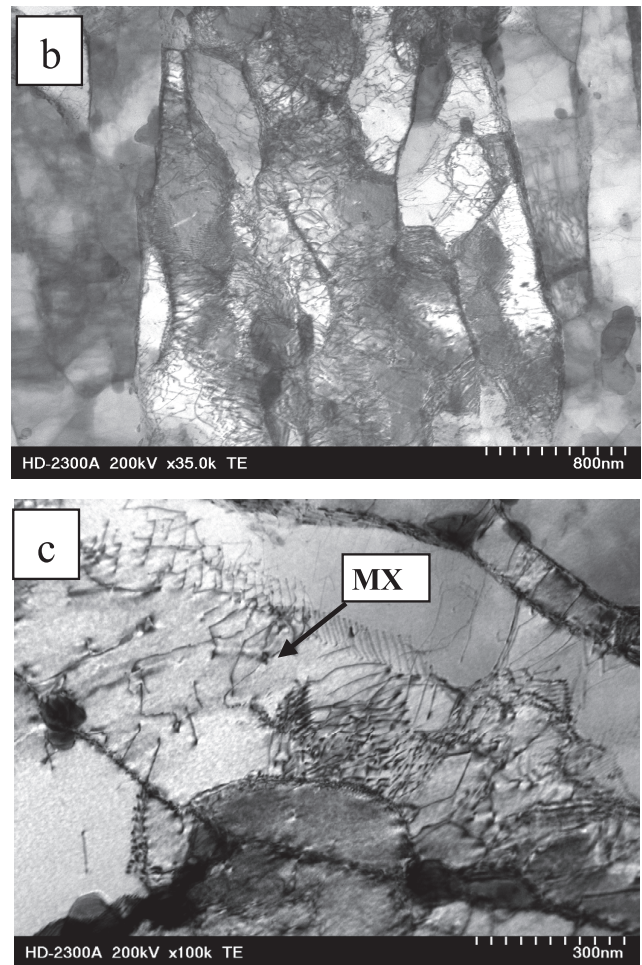


Fig. 11. Tempered martensite substructure of the bend material after QT heat treatment. High dislocation density in the area of numerous subgrains – (a, b). Dispersion precipitates of M23C6 carbides – (a, c) and MX phases on dislocations – (c) are visible

5. Conclusions

1. Based on the research it can be concluded that the tube bend made of the X10CrMoVNb9-1 steel in the analysed process meets the requirements set forth in the PN-EN10216-2 standard. At room temperature, the mechanical characteristics of the bend, i. e. KV, HV10, R_m and $R_{p0.2}$, are comparable to those of the tube material in the as-delivered condition (Table 2).
2. Tests of low-cycle fatigue of the X10CrMoVNb9-1 steel tube material in the as-delivered condition and of the material from the selected bend zones, performed at 600°C within the deformation range $\Delta\varepsilon_f=0.6\%$, showed higher, by circa 40%, low-cycle durability N_f of the bend material as well as lower saturation stress σ_{an} (Fig. 5,6). A similar mechanical behaviour was observed for the bend material within the deformation range $\Delta\varepsilon_f=1.0\%$. Also in this case, the bend material was characterized by a slightly lower (circa 8%) saturation stress σ_{an} . This testifies to

- the decrease of strength properties of the material in the conditions of cyclic loading of an elastic-plastic nature. At the same time, the durability of the bend material, N_f , was about twice as high for each bend zone as it was for the tube material in the as-delivered condition (Fig. 8).
3. Creep tests of the X10CrMoVNb9-1 steel showed a considerably higher steady creep rate (Vu) of the tube material in the as-delivered condition compared to the bend material (Fig. 9), as well as a longer stage II of the steady creep, which results in an increased creep durability of the bend.
4. Based on the presented analyses and discussions of obtained results it should be noted that the parameters of bending and QT heat treatment, adopted in the technological process of fabricating the tube bend from steel X10CrMoVNb9-1, were properly selected. This contributed eventually to the obtaining of the required quality of the tube bend with regard to the geometrical features and mechanical properties.

REFERENCES

- [1] A. Hernas, Materiały i technologie do budowy kotłów nadkrytycznych i spalarni odpadów. Wydawnictwo Stowarzyszenia Inżynierów i Techników Przemysłu Hutniczego w Polsce, Katowice 2009.
- [2] G. Junak, M. Cieśla, Low-cycle fatigue of P91 and P92 steels used in the power engineering industry, "International Conference "Achievements in Mechanical and Materials Engineering", Archives of Materials Science and Engineering **48**, 19-24 (2011).
- [3] Polish Standard PN-EN 10216-2.
- [4] J. Dobrzański, Nowej generacji martenzytyczne stale 9-12% Cr do pracy w warunkach pełzania na elementy krytyczne części ciśnieniowej kotłów energetycznych o nadkrytycznych parametrach pracy; Prace IMŻ 4 (2011).
- [5] <http://www.jachymek.pl/kompleksowe-rozwiazania-w-zakresie-dostaw-rur-dla-energetyki>
- [6] Z. Kowalewski, Zjawisko pełzania metali – eksperyment i modelowanie, Biblioteka Mechaniki Stosowanej, Warszawa 2005.
- [7] A. Hernas, Materiały stosowane w kotłach i turbinach nowej generacji. w monografii pod red. T. Chmielniaka i A. Rusina pt. Maszyny i urządzenia energetyczne węglowych bloków na wysokie parametry pary. Wyd. Politechniki Śl. pp. 42-118., Gliwice 2015.
- [8] A. Hernas, J. Pasternak, S. Fudali, J. Witowski, Właściwości technologiczne nowych materiałów przeznaczonych do budowy kotłów na parametry ultra nadkrytyczne. W pracy zbiorowej pod red. A. Hernasa pt. Procesy niszczenia i powłoki ochronne stosowane w energetyce. Wyd. UKiP J&D Gębka, pp. 240-255. Gliwice 2015.
- [9] W. Kubiński, M. Kuczera, Gięcie rur metalowych na gorąco; Obróbka Plastyczna Metali 4, 23 – 36. (2004).
- [10] W. Kubiński, Wytwarzanie kolan rurowych na gorąco; Hutnik – Wiadomości Hutnicze 12, 467 – 471. (2001).
- [11] J. Pacanowski, Z. Kosowicz Analiza wpływu metody gięcia rur na deformację kolanka rurowego; Rudy i Metale Nieżelazne **R41**, 10, 419 – 423 (1996).
- [12] Z. Hu, J.Q. Li, Computer simulation of pipe-bending processes with small bending radius using local induction heating. Journal of Materials Processing Technology **91**, 75-79 (1999).
- [13] Z. Pater, A. Tofil, FEM simulation of the tube rolling process in Diescher's mill, Advances In Science And Technology Research Journalno **8**, 22, 51-55 (2014).
- [14] Z. Pater, J. Tomczak, J. Bartnicki, M. R. Lovell, P. L. Menezes, Experimental and numerical analysis of helical – wedge rolling process for producing steel balls. International Journal of Machine Tools & Manufacture **67**, 1 – 7. 2013,
- [15] M. Cieśla, R. Findziński, G. Junak, Durability of tube bends made of the 14MoV6-3 steel under low-cycle fatigue conditions and creep at a temperature of 500°C, Solid State Phenomena **226**, 1662-1779, 79-86.
- [16] Z. Pater, Analysis of the helical-wedge rolling process for producing a long stepped shaft, Key Engineering Materials 622-623, 893-898 (2014).

